Published in final edited form as:

Invest Ophthalmol Vis Sci. 2009 December ; 50(12): 5754–5758. doi:10.1167/iovs.09-3398.

Partitioning of the Aqueous Outflow in Rat Eyes

James D. Lindsey, **Anthony Hofer**, **Kristine N. Wright**, and **Robert N. Weinreb**

Sophie and Arthur Brodie Laboratory, Hamilton Glaucoma Center and Department of Ophthalmology, University of California San Diego, La Jolla, California

Abstract

Purpose—To determine the effect of molecular size on the drainage route of dextrans injected into the rat anterior chamber (AC).

Methods—Anesthetized adult rats received monocular AC injections of a mixture of 3-kDa dextran-cascade blue, 40-kDa dextran-Texas red, and 500-kDa dextran-FITC. After exsanguination of the rats 2, 4, 6, 12, 24, or 72 hours later, the eyes, facial lymph nodes, and cervical lymph nodes were isolated, and the total content of each dextran type was determined by spectrofluorometry. Also, lymph nodes were evaluated histologically 4 and 24 hours after AC injection of 40-kDa dextran-FITC.

Results—The speed of tracer exit from the eye varied with 3-kDa dextran > 40-kDa dextran > 500-kDa dextran. No 3-kDa dextran was detected in either facial lymph nodes or cervical lymph nodes at any time point. The average recovery of 40-kDa dextran in the facial and cervical lymph nodes peaked at 52.6% of the amount injected. In contrast, average recovery of 500-kDa dextran in the facial and cervical lymph nodes peaked at 1.8% of amount the injected. Histology showed 40-kDa dextran was mostly contained within lymph node cells at both 4 and 24 hours after injection.

Conclusions—Transport of 40-kDa dextran from the AC to the facial lymph nodes and cervical lymph nodes is markedly more efficient than that of 500-kDa dextran. In contrast, there is negligible transport of 3-kDa dextran. These results demonstrate that different sized aqueous macromolecules can exit the eye by different routes.

The uveoscleral pathway is one of two major routes of the outflow of aqueous humor from the anterior chamber.– Interest in this pathway is growing for several reasons. First, there is decreased uveoscleral outflow with normal aging., Second, although there is some conflicting evidence, elevated IOP in ocular hypertension and exfoliation syndrome glaucoma has been linked to reduced uveoscleral outflow as well as reduced trabecular outflow.,, Finally, topically applied prostaglandin analogues appear to lower IOP by preferentially enhancing uveoscleral outflow.–

Tracer studies have shown that the uveoscleral outflow pathway includes the iris root, ciliary muscle extracellular spaces, anterior choroid, suprachoroidal space, and sclera.,– The course of macromolecules carried by uveoscleral outflow after exiting the sclera is less well

Corresponding author: Robert N. Weinreb, Hamilton Glaucoma Center, University of California San Diego, 9500 Gilman Drive, La Jolla, CA 92093-0946; weinreb@eyecenter.ucsd.edu.

Disclosure: **J.D. Lindsey**, None; **A. Hofer**, None; **K.N. Wright**, None; **R.N. Weinreb**, None

understood. After suprachoroidal injection of Evans blue-labeled albumin, blue staining was reported in rabbit extraocular lymphatic vessels and several associated lymph nodes. Similar experiments have confirmed the migration of labeled albumin (molecular mass = ~67 kDa) or labeled dextrans (40 and 70 kDa) from the anterior chamber to lymph nodes in the face and neck within mice and rats.– In view of the known properties of protein exchange across capillaries, it has been suggested that macromolecules substantially smaller than albumin may exit from the anterior chamber fluid by exchange with blood in uveal tract capillary blood vessels. Evidence supporting this idea is limited. Conversely, histologic tracer studies with 500-kDa dextran suggest that higher molecular mass molecules may be restricted from passage through the uveoscleral outflow pathway. However, the significance of this potential partitioning of aqueous humor proteins is unknown. To assess this possible partitioning of uveoscleral outflow proteins by size, we measured whether there were differences in the migration of 3-, 40-, and 500-kDa–labeled dextrans from the anterior chamber to the facial and cervical lymph nodes.

Methods

All procedures were performed in accordance with the ARVO Statement for the Use of Animals in Ophthalmic and Vision Research. Young adult Long-Evans or Sprague-Dawley rats ranging from 300 to 400 g body weight were maintained in clear plastic enclosures containing pine-shaving bedding and covered loosely with a mesh plastic lid containing an air filter. The rats were provided food and water ad libitum, and were maintained at 21°C in a 12-hour light–dark cycle. Nomenclature for the naming of lymph nodes is according to Tilney.

Tracer Preparation

The tracer cocktail was phosphate-buffered saline (PBS; pH 7.4), containing 1.66 mg/mL each of 3-kDa dextran conjugated to cascade blue, 40-kDa dextran conjugated to Texas red, and 500-kDa dextran conjugated to fluorescein isothiocyanate (FITC), all obtained from Invitrogen (Carlsbad, CA). To prepare stock solutions, each dextran was dissolved in PBS at a concentration of 5.0 mg/mL. Subsequently, the stock solutions were clarified by centrifugation at 14,000*g* for 20 minutes and sterilized by passage through a 0.22-μm syringe filter. Equal amounts of each of these stock solutions were mixed together just before injection (final concentration was 1.66 mg/mL for each dextran type). This concentration was chosen because we were concerned that increased viscosity with higher concentration dextran solutions could make the injections unreliable.

Tracer Injection

Before injection of the tracer, the rats were anesthetized by intraperitoneal injection of a mixture of ketamine (100 mg/kg, Ketaset; Fort Dodge Animal Health, Fort Dodge, IA) and xylazine (10 mg/kg, TranquiVed, Vedco, Inc., St. Joseph, MO). Anesthesia was usually obtained within 4 minutes and absence of tail-pinch reflex was determined before proceeding. A drop of sterile PBS was instilled in each eye to avoid corneal desiccation. Long-Evans rats were used for the spectro-photometric studies. For the histologic analyses,

Sprague-Dawley rats were used to avoid potential autofluorescence from pigment-containing tissues.

The tracer injections were made using a microprocessor-controlled motorized microsyringe fitted with a glass micropipette (UltraMicro-Pump II; World Precision Instruments [WPI], Inc., Sarasota, FL) as described previously. The glass microneedle was made from borosilicate glass tubing (outer diameter, 1.0 mm; inner diameter 0.58 mm; KwikFil; WPI). The tip of the glass microneedle was drawn by pipette puller (P-87; Sutter Instruments, Novato, CA), and a 30 μm-wide beveled tip was produced by a microgrinder (Micropipette Beveler; WPI). The injection volume was 5 μL delivered over 10 minutes and followed by 3 μL of air. The needle was maintained in the eye for a total of 30 minutes before withdrawal. The injected air bubble minimized the reflux of tracer through the corneal perforation. The animals were allowed to recover in an incubator warmed to 33°C. A separate group of four rats received anterior chamber injection of 15-μg 40-kDa lysine fixable dextran-FITC. Lymph nodes from these rats were examined histologically at 4 and 24 hours after the injection. Three replicate experiments were performed with one animal at each of the following postinjection survival times: 1, 2, 4, 6, 12, 24, and 72 hours. For each experiment, a new dilution of the dextran mixture from stock solutions was prepared and new standard curves were generated.

Spectrofluorometric Analyses

At the end of the survival period, the rats were killed by CO_2 inhalation and then exsanguinated by using 60 mL of PBS. The facial and cervical lymph nodes plus the whole eyes were quickly isolated, weighed, and stored frozen. The tissues were quickly thawed in 200 μL of Hanks' balanced salt solution (HBSS) per 100 mg tissue and homogenized with a glass pestle homogenizer. The homogenate was then centrifuged at 14,000*g* for 30 minutes, and then the supernatant was assayed with a diode array spectrofluorometer (Nanodrop ND-3300; Thermo Scientific, Wilmington, DE). Excitation and emission specifications for each tracer were as follows: 3-kDa casacade blue 400 UV light/420 nM, 40-kDa Texas red 595 white light/615 nm, and 500-kDa FITC 495 blue light/518 nm. Concentration for each tracer type within the supernatant was determined by comparison with standard curves generated by spiking lymph node homogenates generated from rats that did not receive tracer injection. The standard curve for each respective dextran was 50, 25, 12.5, 6.25, 3.125, 1.56, and 0.78 μg/mL. Correlation coefficients for the curves for each standard were >0.98. Background fluorescence signal measured in the unspiked naïve rat lymph node supernatants was subtracted from all measurements. Spike recovery tests also confirmed that for each of the tracers, there was negligible cross-talk signal from the other tracers with those excitation and emission settings.

Histologic Analysis

At 4 and 24 hours after injection with 40-kDa dextran conjugated to FITC and to lysine, the rats were killed by CO_2 inhalation. The lysine allowed cross-linking of the dextran to structural proteins on exposure to aldehyde fixative. The vascular bed was rinsed by transcardial perfusion with PBS followed by 2% paraformaldehyde freshly prepared in 0.12 M phosphate buffer (pH 7.4). After dissection, lymph nodes were fixed an additional 3 hours

in fixative, dehydrated through a graded ethanol series, and embedded in polyester wax. Serial 6-μm-thick sections were cut and then mounted on gelatin-coated glass slides. The sections were examined by fluorescence microscope with fluorescein excitation and emission filters, and images were captured with a cooled charged-coupled-device digital camera (Spot Camera; Diagnostic Instruments, Sterling Heights, MI).

Analysis Considerations and Statistics

Investigators in prior studies have noted that although the general organization of the lymphatic system is constant, there is often considerable individual variability in the structure and labeling of extraocular lymphatic vessels and their downstream nodes after injection of tracers.,, Thus, emphasis was placed on general conclusions. Another consideration is that the size of dextrans within commercial preparations falls within a range that varies according to a bell curve. In a previous study in which a mixture of commercial dextran preparations was analyzed by gel filtration, the peaks for 4- and 40-kDa dextran were readily distinguished, although some overlap of the lower portion of the peaks was present.

Experimental results were analyzed by analysis of variance. $P < 0.05$ was considered significant.

Results

Exit from the Eye

After intracameral injection of the tracer, decline in the amount of tracer remaining in the eye depended on the size of the tracer. Three-kilodalton dextran was present in the eyes with survival times of 2 to 6 hours but was absent in eyes with greater survival times (Fig. 1). The presence of 40-kDa dextran in the injected eye was observed with survival times up to 24 hours but was not observed at 72 hours after injection. In contrast, residual 500-kDa dextran was observed at all time points tested. There was a marked decline in the amount of 500-kDa dextran remaining between 6 and 12 hours after injection.

Size-Dependent Migration of Dextran in Facial and Cervical Lymph Nodes

There was no recovery of 3-kDa dextran in the lymph nodes of any animal at any time point (data not shown). The recovery of 40-kDa dextran (Fig. 2) and 500-kDa dextran (Fig. 3) varied considerably among the animals at each time point. Nevertheless, two general patterns emerged. First, there was much greater recovery of 40-kDa dextran than the 500-kDa dextran in both lymph node types ($P < 0.05$). And second, the total recovery of 40-kDa dextran exceeded the total recovery of 500-kDa dextran ($P < 0.05$). These differences are more readily apparent when the means of the data across the cohorts at each time point are compared (Fig. 4). The general pattern for the 40-kDa dextran was to gradually increase in the lymph nodes with survival times up to 12 hours and to gradually decline after 12 hours. The peak recovery observed at 12 hours after injection was 53% of the total injected. In contrast, the recoveries of 500-kDa dextran were similar to each other at each of the time points and were always less than 3% of the total injected.

Histologic Analysis

Examination of cervical and facial lymph nodes 4 and 12 hours after injection of 40-kDa lysine fixable dextran-FITC revealed a staining pattern largely within cellular elements within the subcapsular sinus of the lymph node (Fig. 5). The proportion of cells stained and the intensity of staining were both greater at 24 hours after injection than at 4 hours. Staining in the cervical lymph nodes was similar (data not shown). Prior double-staining investigations have demonstrated that cells in lymph nodes labeled by 40-kDa dextran injection into the anterior chamber include macrophages, dendritic cells, antigen-presenting cells, and T lymphocytes.

Discussion

This study provides direct evidence that different sized aqueous macromolecules exit by different routes. Consistent with previous studies, we observed that 40-kDa dextran gradually migrated from the eye to the facial and cervical lymph nodes over the 24 hours after injection into the anterior chamber. A different pattern was observed with the 3-kDa dextran in which more than 97% had exited the eye within the first 2 hours after injection and none was ever observed in the lymph nodes. In contrast, 7% to 10% of the 500-kDa dextran remained in the eye for the first 6 hours after injection, and only approximately 2% was found in the lymph nodes at any time during the entire 72-hour examination period. Histologic examination of the lymph nodes demonstrated that most of the 40-kDa dextran was taken up into cells of the lymph nodes. This is similar to the uptake of dextran into cells within the outflow pathways of the eye previously observed after anterior chamber injections of dextrans.,

A significant proportion of each of the injected dextrans did not migrate to the lymph nodes. In anticipation of this, blood samples were obtained from each of the animals in this study at the time of death. However, with the methods used in the present study, there was insufficient signal to measure the concentration of any of the three dextrans within the serum from these samples. In view of previous studies that demonstrated the uptake of fluorescent dextran by lymphocytes and cortical spleen cells,, it is possible that those dextrans migrating to the blood by trabecular outflow or capillary exchange were cleared from the serum before sample collection. Because autofluorescence is present within erythrocytes in many tissue types, it may be best to further pursue this issue experimentally using radioactively labeled dextrans.

It is unlikely that certain sized dextrans may have been taken up selectively by the terminal lymphatics. Tracer studies indicate the formation of lymph at lymphatic termini that captures macromolecules and microparticles ranging up to ~500 nm in size. Moreover, mass spectrometer studies have identified lymph proteins as small as 2.5 kDa., Thus, it is probable that if they were present near the lymphatic terminals, each of the 3-, 40-, and 500-kDa dextrans would have been readily taken up by lymph terminals.

In view of the above considerations, several conclusions can be made regarding differences in the general outflow characteristics of different sized dextran tracers. As summarized in Table 1, migration of 40-kDa dextran out of the eye was complete between 24 and 72 hours

after injection. This result is in general agreement with prior descriptions of bulk uveoscleral outflow in rabbits and monkeys. The present and prior histologic studies indicate that movement of this dextran from the eye and through the lymph nodes involves local uptake and release of some of the label by various cell types along the path from the anterior chamber to the lymph nodes, a process that is likely to prolong its outflow.

It is interesting that the amount of 40-kDa dextran present in either the lymph nodes 12 hours after injection was approximately 52% of the injected total. Considering that 7% of the injected dextran was still in the eye, this finding could indicate that uveoscleral outflow was approximately 56% of total out-flow (52/93; 56%). This proportion present within the young adult rats used in this study is similar to the amount of uveoscleral outflow observed in prior studies of normal young human eyes.

In contrast to 40-kDa dextran, 3-kDa dextran was observed only in the injected eye, for only the first 6 hours, and more than 97% was unaccounted for (not in the eye or in lymph nodes) by the second hour after injection. This suggests that the 3-kDa dextran generally exits by a route that diverges in speed and possibly in route from bulk uveoscleral outflow. Also different from 40-kDa dextran, approximately 7% to 10% of the injected 500-kDa dextran remained in the eyes during the first 6 hours and less than 3% was observed in the lymph nodes at any of the time points after injection. Since an earlier histologic study from our laboratory reported bright accumulation of 500-kDa fluorescent dextran in the region of the ciliary body 20 minutes after AC injection, the present results suggest that the spaces between ciliary muscle cells became clogged shortly after the injection and that most of the 500-kDa dextran may have been diverted from entering the posterior uveoscleral outflow pathway. Nevertheless, a small portion of the 500-kDa dextran was able to migrate to the facial and ciliary lymph nodes.

In conclusion, the results of this study provide evidence that different sized aqueous macromolecules can exit by different routes. If this conclusion is correct, preferential targeting of therapeutics to different ocular tissues may be achieved by varying molecular size. These results may have important implications for protein-based therapy for eye disease.

Acknowledgments

Supported in part by National Eye Institute Grant EY05990 (RNW).

References

1. Bill A. The drainage of albumin from the uvea. Exp Eye Res. 1964; 3:179–187. [PubMed: 14211921]
2. Bill A. Uveoscleral drainage of aqueous humor: physiology and pharmacology. Prog Clin Biol Res. 1989; 312:417–427. [PubMed: 2678147]
3. Nilsson SF. The uveoscleral outflow routes. Eye. 1997; 11:149–154. [PubMed: 9349404]
4. Toris CB, Yablonski ME, Wang YL, Camras CB. Aqueous humor dynamics in the aging human eye. Am J Ophthalmol. 1999; 127:407–412. [PubMed: 10218693]
5. Gabelt BT, Kaufman PL. Changes in aqueous humor dynamics with age and glaucoma. Prog Retin Eye Res. 2005; 24:612–637. [PubMed: 15919228]

6. Yablonski ME, Cook DJ, Gray J. A fluorophotometric study of the effect of argon laser trabeculoplasty on aqueous humor dynamics. Am J Ophthalmol. 1985; 99:579–582. [PubMed: 4003496]
7. Toris CB, Camras CB, Yablonski ME. Aqueous humor dynamics in ocular hypertensive patients. J Glaucoma. 2002; 11:253–258. [PubMed: 12140404]
8. Johnson TV, Fan S, Camras CB, Toris CB. Aqueous humor dynamics in exfoliation syndrome. Arch Ophthalmol. 2008; 126:914–920. [PubMed: 18625936]
9. Crawford K, Kaufman PL. Pilocarpine antagonizes prostaglandin $F_{2\alpha}$-induced ocular hypotension in monkeys: evidence for enhancement of uveoscleral outflow by prostaglandin $F_{2\alpha}$. Arch Ophthalmol. 1987; 105:1112–1116. [PubMed: 3477218]
10. Gabelt BT, Kaufman PL. Prostaglandin $F_{2\alpha}$ increases uveoscleral outflow in the cynomolgus monkey. Exp Eye Res. 1989; 49:389–402. [PubMed: 2792235]
11. Toris CB, Camras CB, Yablonski ME. Effects of PhXA41, a new prostaglandin $F_{2\alpha}$ analog, on aqueous humor dynamics in human eyes. Ophthalmology. 1993; 100:1297–1304. [PubMed: 8371915]
12. Weinreb RN, Toris CB, Gabelt BT, Lindsey JD, Kaufman PL. Effects of prostaglandins on the aqueous humor outflow pathways. Surv Ophthalmol. 2002; 47(suppl 1):S53–S64. [PubMed: 12204701]
13. Kaufman PL. Enhancing trabecular outflow by disrupting the actin cytoskeleton, increasing uveoscleral outflow with prostaglandins, and understanding the pathophysiology of presbyopia interrogating Mother Nature: asking why, asking how, recognizing the signs, following the trail. Exp Eye Res. 2008; 86:3–17. [PubMed: 18053986]
14. Bill A. Aqueous humor dynamics in monkeys (Macaca irus and Cercopithecus ethiops). Exp Eye Res. 1971; 11:195–206. [PubMed: 5001096]
15. Inomata H, Bill A, Smelser GK. Aqueous humor pathways through the trabecular meshwork and into Schlemm's canal in the cynomolgus monkey (Macaca irus): an electron microscopic study. Am J Ophthalmol. 1972; 73:760–789. [PubMed: 4623937]
16. Inomata H, Bill A. Exit sites of uveoscleral flow of aqueous humor in cynomolgus monkey eyes. Exp Eye Res. 1977; 25:113–118. [PubMed: 410651]
17. Hoffmann F, Zhang EP, Mueller A, et al. Contribution of lymphatic drainage system in corneal allograft rejection in mice. Graefes Arch Clin Exp Ophthalmol. 2001; 239:850–858. [PubMed: 11789866]
18. Camelo S, Shanley A, Voon AS, McMenamin PG. The distribution of antigen in lymphoid tissues following its injection into the anterior chamber of the rat eye. J Immunol. 2004; 172:5388–5395. [PubMed: 15100279]
19. Camelo S, Kezic J, Shanley A, Rigby P, McMenamin PG. Antigen from the anterior chamber of the eye travels in a soluble form to secondary lymphoid organs via lymphatic and vascular routes. Invest Ophthalmol Vis Sci. 2006; 47:1039–1046. [PubMed: 16505039]
20. Alm A. Uveoscleral outflow. Eye. 2000; 14:488–491. [PubMed: 11026978]
21. Bernd AS, Aihara M, Lindsey JD, Weinreb RN. Influence of molecular weight on intracameral dextran movement to the posterior segment of the mouse eye. Invest Ophthalmol Vis Sci. 2004; 45:480–484. [PubMed: 14744888]
22. Tilney NL. Patterns of lymphatic drainage in the adult laboratory rat. J Anat. 1971; 109:369–383. [PubMed: 5153800]
23. Lindsey JD, Weinreb RN. Identification of the mouse uveoscleral outflow pathway using fluorescent dextran. Invest Ophthalmol Vis Sci. 2002; 43:2201–2205. [PubMed: 12091417]
24. Toris CB, Gregerson DS, Pederson JE. Uveoscleral outflow using different-sized fluorescent tracers in normal and inflamed eyes. Exp Eye Res. 1987; 45:525–532. [PubMed: 2448157]
25. Lynch PM, Delano FA, Schmid-Schönbein GW. The primary valves in the initial lymphatics during inflammation. Lymphat Res Biol. 2007; 5:3–10. [PubMed: 17508898]
26. Interewicz B, Olszewski WL, Leak LV, Petricoin EF, Liotta LA. Profiling of normal human leg lymph proteins using the 2-D electrophoresis and SELDI-TOF mass spectrophotometry approach. Lymphology. 2004; 37:65–72. [PubMed: 15328759]

27. Jones M, Fusaro VA, Ross SJ, Zhao Y, Petricoin EF 3rd. Proteomic analysis of lymph. Proteomics. 2004; 4:753–765. [PubMed: 14997497]

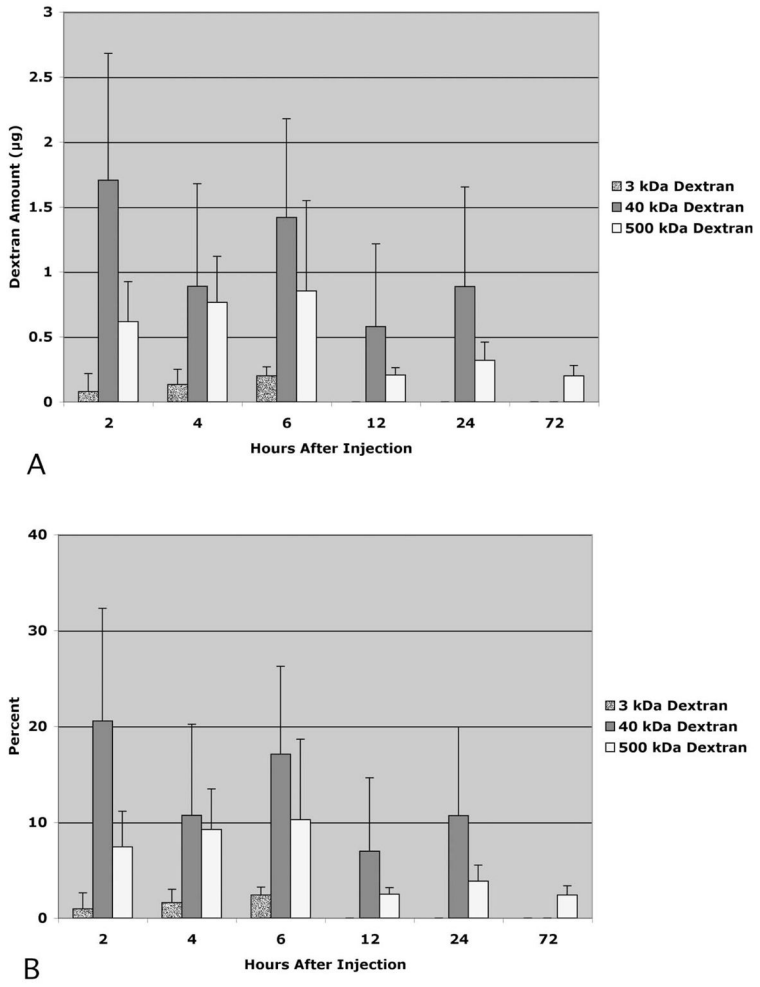

Figure 1.

Portion of each dextran present in eyes 2 to 72 hours after injection expressed as total recovered (**A**) and as a percentage of the total injected (**B**). *n* = 3 eyes per time point. Error bars, SD.

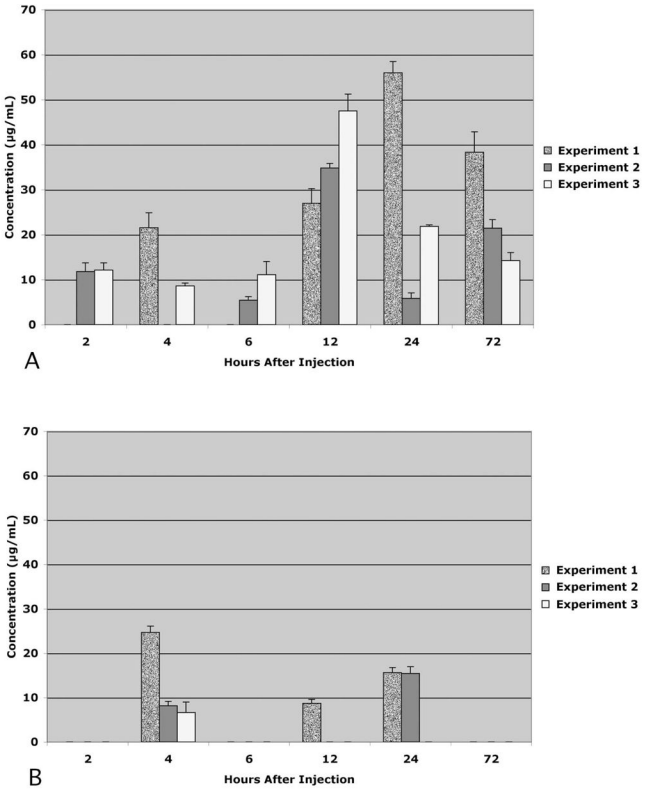

Figure 2.

Distribution of 40-kDa dextran in the facial lymph nodes (**A**) and cervical lymph nodes (**B**) 2 to 72 hours after injection. Data expressed as the concentration within lymph node homogenate supernatants. In each experiment, there was one animal per time point. Altogether, there were three experiments. Each data bar reflects the mean of quadruplicate measurements in each animal. Error bars, SD.

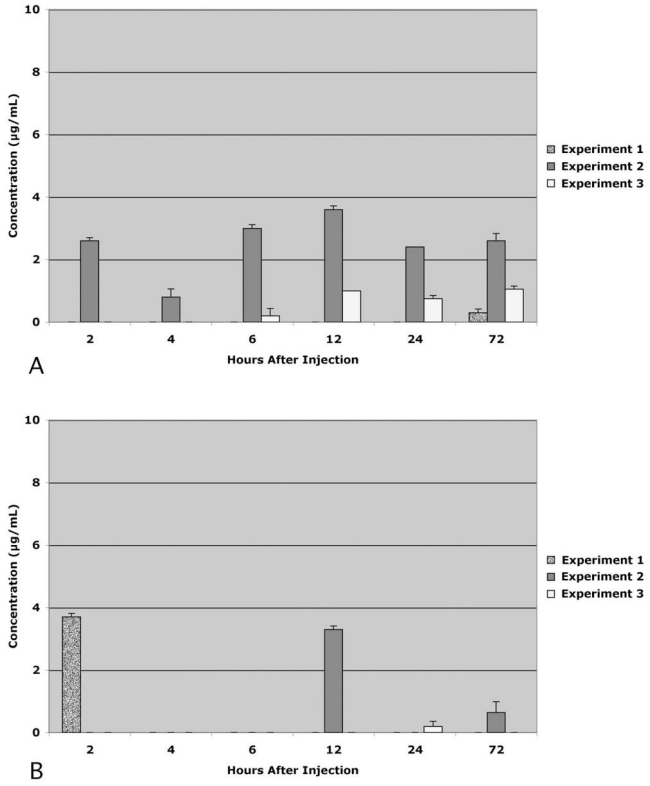

Figure 3.

Distribution of 500-kDa dextran in the facial lymph nodes (**A**) and cervical lymph nodes (**B**) 2 to 72 hours after injection into the eye. Data expressed as concentration within lymph node homogenate supernatants. Each data bar reflects the mean of quadruplicate measurements from each animal. Error bars, SD. Note that the scales differ from those in Figure 2.

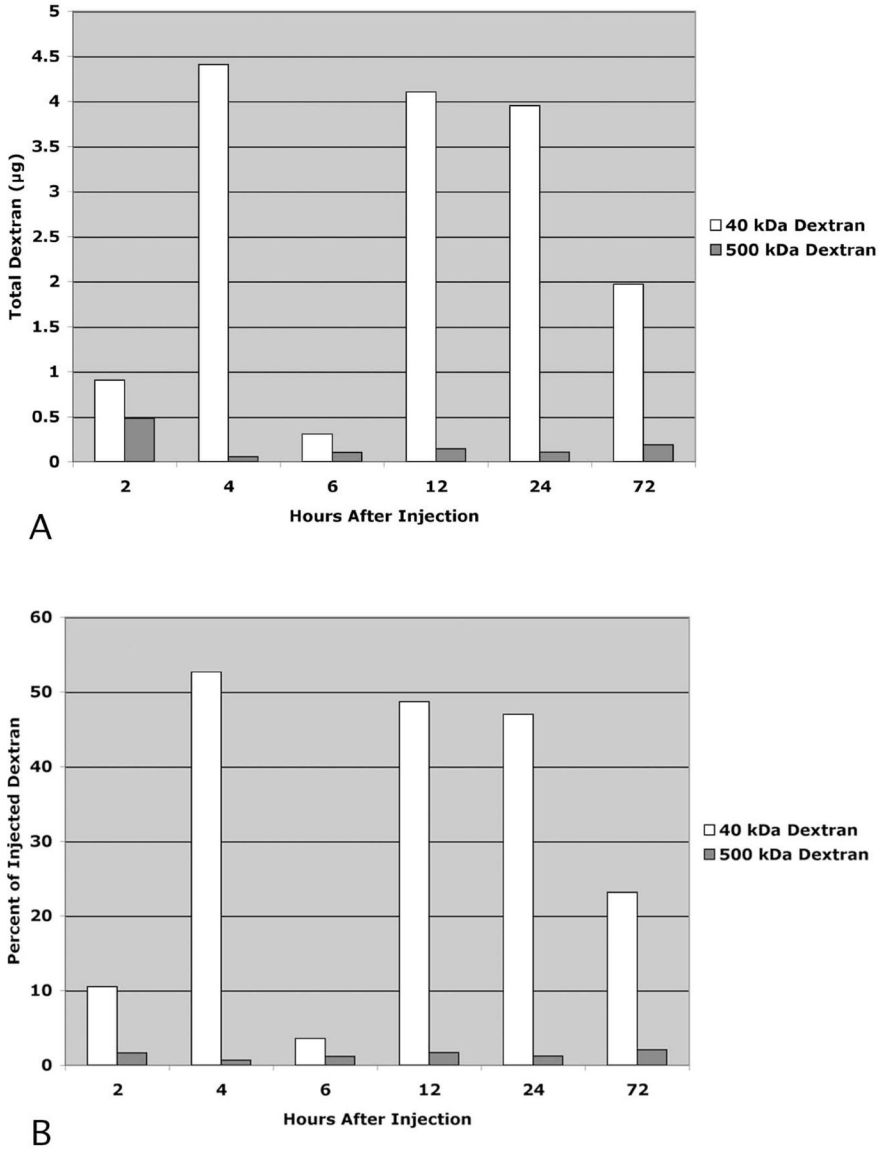

Figure 4.

Comparison of the sum of each detected dextran within the facial and cervical lymph nodes 2 to 72 hours after injection. Data expressed as total dextran recovered (**A**) and as a percentage of injected dextran (**B**). $n = 3$ rats per experimental condition.

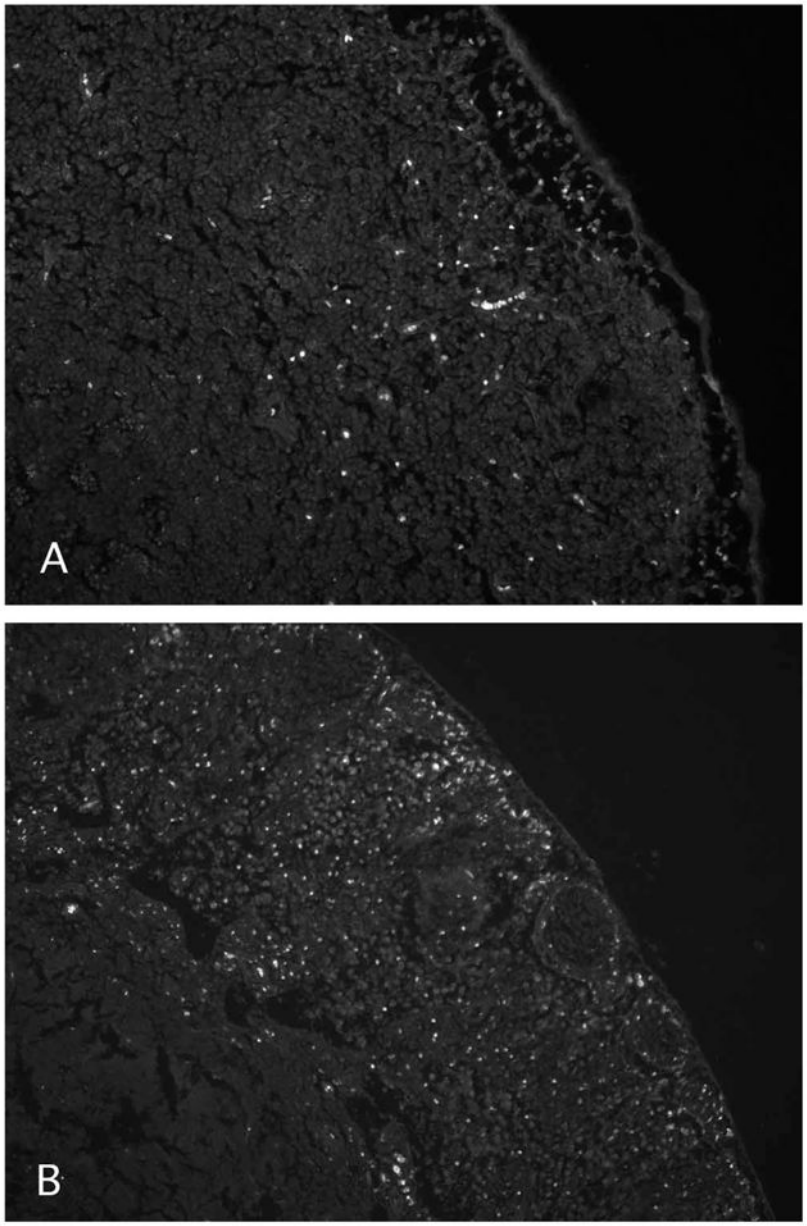

Figure 5.

Distribution of fluorescence in the subcapsular sinus of facial lymph nodes at 4 (**A**) or 24 (**B**) hours after anterior chamber injection of 40-kDa lysine fixable dextran conjugated to FITC. Magnification, ×220.

Table 1

Dextran Distribution Differences Shown as Percent of Total Injected

	Hours after Injection	Eye	Lymph Nodes*	Total	Unaccounted
40 kDa	2	20.6	10.5	31.1	68.9
	4	10.7	52.6	63.3	36.7
	6	17.1	3.6	20.7	79.3
	12	7.0	52.1	59.0	41.0
	24	10.7	47.0	57.7	42.3
	72	0	23.2	23.2	76.8
3 kDa	2	1.0	0	1.0	99.0
	4	1.6	0	1.6	98.4
	6	2.4	0	2.4	97.6
	12	0	0	0	100
	24	0	0	0	100
	72	0	0	0	100
500 kDa	2	7.4	1.8	9.1	90.9
	4	9.2	0.7	9.9	90.1
	6	10.3	1.2	11.5	88.5
	12	2.5	1.6	4.1	95.9
	24	3.9	1.2	5.1	94.9
	72	2.4	2.4	4.8	95.2

*Sum of dextran within the facial and cervical lymph nodes.

Invest Ophthalmol Vis Sci. Author manuscript; available in PMC 2017 November 06.